Research Article | Vol. 8, No. 9 | 1 Sep 2018 | OPTICAL MATERIALS EXPRESS 2654

Optical Materials EXPRESS

Shaping the fundamental and second harmonic beams using patterned facets in lithium triborate

DANVEER SINGH,* ROY SHILOH, AND ADY ARIE

School of Electrical Engineering, Tel Aviv University, Tel Aviv 69978, Israel
**danveersingh@mail.tau.ac.il*

Abstract: We demonstrate a new method for high resolution patterning of the facets of a nonlinear crystal, LiB_3O_5, based on lithographic exposure of its anti-reflection coating layer, followed by ion beam milling. This crystal is attractive for high intensity frequency conversion due to its high damage threshold. We demonstrate an application of our patterning method for shaping the fundamental beam, as well as the second harmonic beam that is generated in the crystal. We fabricated six different phase masks that generated the following beam profiles in both wavelengths: on- and off-axis high order Hermite-Gaussian beam, Airy beam, vortex beam, lens and a periodic Bragg grating. Such an optical device opens up new possibilities for compact beam shaping in high power nonlinear interaction in a broad range of frequencies.

OCIS codes: (190.2620) Harmonic generation and mixing; (190.4360) Nonlinear optics, devices; (050.1380) Binary optics; (220.0220) Optical design and fabrication.

References and links

1. D. L. S. Fred, M. Dickey, T. E. Lizotte, S. C. Holswade, *Laser Beam Shaping Applications* (CRC Press, 2006).
2. J. R. Kurz, A. M. Schober, D. S. Hum, A. J. Saltzman, and M. M. Fejer, "Nonlinear physical optics with transversely patterned quasi-phase-matching gratings," IEEE J. Sel. Top. Quantum Electron. **8**(3), 660–664 (2002).
3. Y. Q. Qin, C. Zhang, Y. Y. Zhu, X. P. Hu, and G. Zhao, "Wave-front engineering by Huygens-Fresnel principle for nonlinear optical interactions in domain engineered structures," Phys. Rev. Lett. **100**(6), 063902 (2008).
4. T. Ellenbogen, A. Ganany-Padowicz, and A. Arie, "Nonlinear photonic structures for all-optical deflection," Opt. Express **16**(5), 3077–3082 (2008).
5. T. Ellenbogen, N. Voloch-Bloch, A. Ganany-Padowicz, and A. Arie, "Nonlinear generation and manipulation of airy beams," Nat. Photonics **3**(7), 395–398 (2009).
6. A. Shapira, I. Juwiler, and A. Arie, "Nonlinear computer-generated holograms," Opt. Lett. **36**(15), 3015–3017 (2011).
7. A. Shapira, R. Shiloh, I. Juwiler, and A. Arie, "Two-dimensional nonlinear beam shaping," Opt. Lett. **37**(11), 2136–2138 (2012).
8. A. Aadhi, N. A. Chaitanya, M. V. Jabir, P. Vaity, R. P. Singh, and G. K. Samanta, "Airy beam optical parametric oscillator," Sci. Rep. **6**(1), 25245 (2016).
9. A. Shapira, A. Libster, Y. Lilach, and A. Arie, "Functional facets for nonlinear crystals," Opt. Commun. **300**, 244–248 (2013).
10. S. Lightman, R. Gvishi, G. Hurvitz, and A. Arie, "Shaping of light beams by 3D direct laser writing on facets of nonlinear crystals," Opt. Lett. **40**(19), 4460–4463 (2015).
11. Y. M. Andreev, M. Naftaly, J. F. Molloy, A. E. Kokh, G. V. Lanskii, V. A. Svetlichnyi, V. F. Losev, N. G. Kononova, and K. A. Kokh, "LBO: Optical properties and potential for THz application," Laser Phys. Lett. **12**(11), 115402 (2015).
12. Y. Furukawa, S. A. Markgraf, M. Sato, H. Yoshida, T. Sasaki, H. Fujita, T. Yamanaka, and S. Nakai, "Investigation of the bulk laser damage of lithium triborate, LiB_3O_5, single crystals," Appl. Phys. Lett. **65**(12), 1480–1482 (1994).
13. W.-H. Lee, "Binary computer-generated holograms," Appl. Opt. **18**(21), 3661–3669 (1979).
14. L. Allen, M. W. Beijersbergen, R. J. C. Spreeuw, and J. P. Woerdman, "Orbital angular momentum of light and the transformation of Laguerre-Gaussian laser modes," Phys. Rev. A **45**(11), 8185–8189 (1992).
15. B. E. A. Saleh and M. C. Teich, *Fundamentals of Photonics*, 2nd Edition (Wiley, 2007), p. 1200.
16. G. A. Siviloglou, J. Broky, A. Dogariu, and D. N. Christodoulides, "Observation of accelerating Airy beams," Phys. Rev. Lett. **99**(21), 213901 (2007).
17. D. G. Grier, "A revolution in optical manipulation," Nature **424**(6950), 810–816 (2003).

#331093 https://doi.org/10.1364/OME.8.002654
Journal © 2018 Received 7 May 2018; revised 20 Jun 2018; accepted 5 Jul 2018; published 14 Aug 2018

Optical Materials EXPRESS

18. J. Broky, G. A. Siviloglou, A. Dogariu, and D. N. Christodoulides, "Self-healing properties of optical Airy beams," Phys. Rev. Lett. Contemp. Phys **58**(46), 1499–1501 (1987).
19. J. Feng, C. Zhou, B. Wang, J. Zheng, W. Jia, H. Cao, and P. Lv, "Three-port beam splitter of a binary fused-silica grating," Appl. Opt. **47**(35), 6638–6643 (2008).
20. R. Schnabel, A. Bunkowski, O. Burmeister, and K. Danzmann, "Three-port beam splitters-combiners for interferometer applications," Opt. Lett. **31**(5), 658–660 (2006).
21. R. W. Gerchberg and W. O. Saxton, "A practical algorithm for the determination of phase from image and diffraction plane pictures," Optik (Stuttg.) **35**(2), 237–246 (1972).

1. Introduction

Nonlinear frequency conversion in quadratic nonlinear crystals is widely used to generate coherent radiation in wavelengths in which compact and efficient sources are not available. In many applications, such as material processing, photolithography, medical, and scientific research [1], the generated beam in the nonlinear crystal has to be shaped using conventional optical elements placed beyond the exit facet of the crystal, e.g. lenses, filters, spatial light modulators, mode converters, etc. These optical elements often consume large work space, they induce unwanted mechanical instabilities and increase the overall cost of the system.

An alternative method to overcome these problems is to integrate the beam shaping process within the nonlinear crystal. In the past, in order to achieve the desired beam profile, the second-order nonlinear coefficient has been spatially modulated to manipulate the beam profile in a variety of examples such as focusing [2,3], steering [4] and shaping [5–8]. However, this approach holds several drawbacks; in particular, the difficulty to achieve efficient phase matching along with shaping of the beam in two transverse dimensions. Moreover, it is limited only to crystals that can be used in quasi-phase matched processes, mainly fairly thin (~1 mm thickness) ferroelectric crystals having relatively low intensity damage threshold and limited spectral coverage at ultraviolet wavelengths.

An alternative is the direct functionalization of the facet of the nonlinear crystal. This has been previously demonstrated by adding a metal layer which was then patterned by focused ion beam milling, in order to generate a binary amplitude mask [9] or by direct three-dimensional printing of phase masks in a polymer that was added to the facet of the crystal [10]. Whereas these two techniques enabled arbitrary shaping of beams that were generated in the nonlinear crystal, they are still limited to low power applications – in the first technique owing to absorption and losses in the metal layer of the amplitude mask, and in the second method owing to the limited damage threshold of the polymer that is used in the printing process.

In this letter, we demonstrate a new method for shaping beams in nonlinear processes, that is suitable for very high-intensity applications. It is based on milling phase masks directly into the anti-reflection coating layer at the exit facet of a lithium triborate LiB_3O_5 (LBO) crystal. LBO is characterized by a wide transparency range (155–3200 nm), extremely high laser-induced damage threshold at 1064nm wavelength (45 GW/cm^2 for 1ns pulses) and low linear optical absorption [11,12]. Such properties are highly desired in high power industrial applications.

2. Fabrication process

The LBO crystal we used (Raicol crystals) had dimensions of 7×3×3 mm^3 and was cut for type-I critical second harmonic phase matching of 1064 nm light. The input and output facets were protected with a 600 nm thick anti-reflective coating for 1064 nm light, consisting of a stack of layers of silicon dioxide (SiO_2) and hafnium dioxide (HfO_2). The crystal was placed in a special hollow cylindrical holder with its exit facet facing up. The holder was designed to be compatible with our spin-coater, where we found that transversely orienting the crystal slightly-off relative to the rotation axis allowed for a more homogeneous spread of the resist, probably due to the higher momentum, where otherwise the small surface area of the facet incurs an oblate shape of the resist. Figure 1(a) illustrates schematically the fabrication

Optical Materials EXPRESS

process. Two types of lithographic processes were separately employed: in the UV process, we exposed the mask onto AZ1518 photoresist. In the e-beam process, we wrote the mask directly onto PMMA augmented with an additional conductive layer (Electra 92 AR-PC 5090.02, not shown). Following development, the coating layer of the crystal was etched through the mask using a broad-beam ion dry etching machine (AJA Ion miller, Phase 2J). The remaining resist was then removed with acetone and ultrasonic treatment. In order to assess the optical quality of the patterned crystal, we used an Olympus LEXT 4000 confocal microscope.

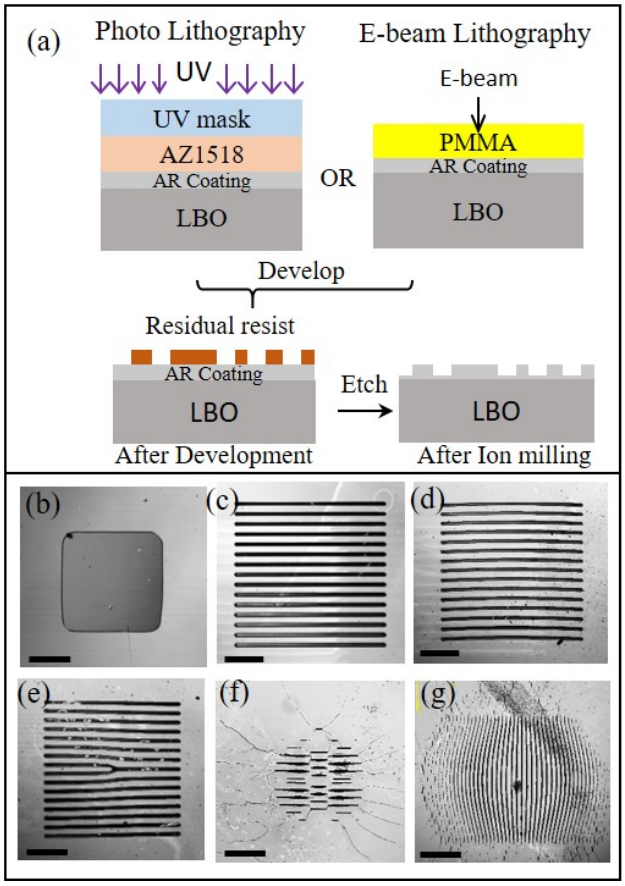

Fig. 1. (a) Schematic of the fabrication process of binary patterns using lithographic methods. (b-g) Confocal microscopic images of milled structures on the LBO facet, namely (b) binary phase step; (c) Bragg grating; (d) lens; (e) fork grating; (f) Hermite-Gauss of order 1,2; (g) Two-dimensional Airy beam. All scale bars are 40 μm.

3. Results and discussion

3.1 On-axis beam shaping

We first tested the fabrication process by generating a π-phase step, as shown in Fig. 2. This structure is useful for on-axis generation of HG_{10}-like beam, which is characterized by a π-phase jump on axis. The accumulated phase of the wave for a step of height *h(x, y)* is

$$\Phi(x,y)=\frac{2\pi(n-n_{air})\times h(x,y)}{\lambda} \quad (1)$$

Optical Materials EXPRESS

Here, n and n_{air} represent the refractive indices of the anti-reflection coating and air, respectively and λ is the operating wavelength. We estimate that the refractive index of the multilayer coating as the average of the refractive indices of HfO_2 and SiO_2, i.e ~1.7. Setting $h = \lambda / 2(n - n_{air})$ ~380 nm we obtain a phase step of approximately π radians for the second harmonic (SH) wavelength of 532 nm. Note that the accumulated phase for the fundamental frequency (FF) is approximately π/2. The generation of HG_{10}-like mode was obtained by illuminating the edge of the π-phase step square with the beam waist, as shown in Fig. 2(a) and Fig. 2(b), so that half of the beam accumulates the π phase shift. The microscopic image of the fabricated phase step is shown in Fig. 1(b). Figure 2 shows the measured (top), and simulated (bottom) SH Fig. 2(c) and FF Fig. 2(d) beams. The experimental intensity measurements exhibit good correlation (>80%) with simulation, where we attribute the difference mainly due to non-uniform milling of π-phase step because of fabrication errors.

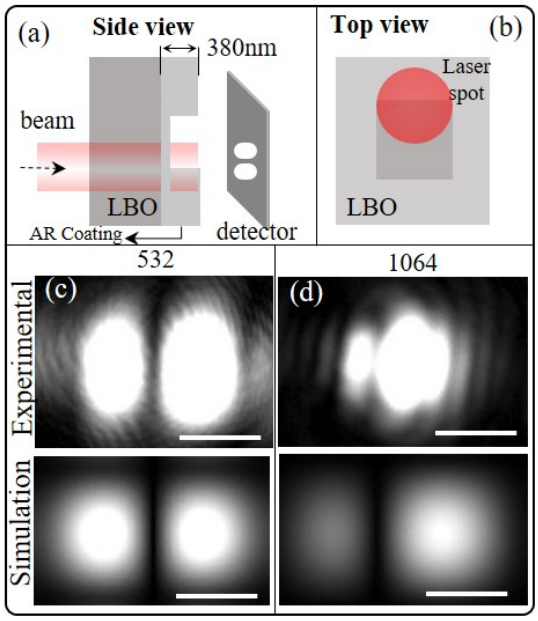

Fig. 2. (a, b) Schematic illustration of beam positioning on the π phase-step structure which determines the spatial distribution of HG_{10} mode. Simulated (bottom) and measured (top) for (c) SH and (d) FF of the generated HG_{10}. The scale bar is 150μm.

3.2 Off-axis beam shaping using a binary phase mask

In order to realize more complex beam shaping, the next step was to design and fabricate off-axis binary phase masks on the crystal's facet. These are computer generated holograms (CGH), and the design was based on the method of Lee [13]. Whereas Lee's original coding scheme was based on binary amplitude modulation, here we perform binary phase modulation so that the facet transmission function is given by

$$T(x,y) = \exp\{\frac{\Delta\Phi}{2}[1 + sign[\cos(\frac{2\pi}{\Lambda} + \varphi(x,y)) - \cos(\pi q(x,y))]]\} \qquad (2)$$

Here, $q(x, y)$ is defined by $A(x,y) = sin(\pi q(x,y))$. $A(x,y)$ and $\varphi(x,y)$ are amplitude and the phase of the Fourier transform of the desired beam profile in the first order of diffraction. Λ is a grating period of 10μm. The phase step $\Delta\Phi$ is defined by the etching process, in a similar manner to what we described for the simple phase-step. The microscopic images of five different fabricated off-axis hologram patterns are shown in Fig. 1(c)–1(g). These

Optical Materials EXPRESS

include: a periodic Bragg grating, a focusing lens, a fork grating for generating Laguerre-Gauss-like beams [14] with one topological charge, Hermite-Gauss-like beam of order 1,2 [15], and a two-dimensional Airy beam [16]. The generated beams have interesting properties. For example, the Hermite-Gaussian beam is self-similar and maintains its shape as it expands owing to diffraction. This is also the case with Laguerre-Gaussian modes, though these also have a non-zero azimuthal index such that they carry orbital angular momentum and hence could be useful for spatial manipulations of micro-particles by light [17]. The Airy beam exhibits self-acceleration and self-healing properties [18].

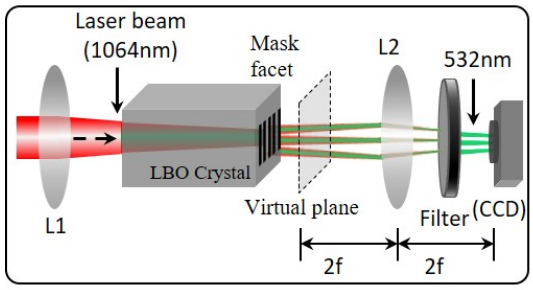

Fig. 3. Schematic of the optical setup. L1 and L2 are lenses. A band pass filter was used to remove the pump wavelength from the generated second harmonic frequency.

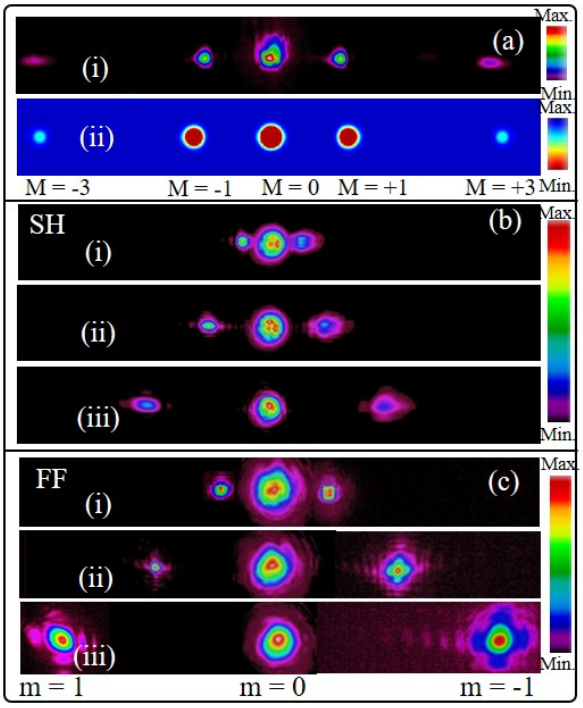

Fig. 4. (a) Diffraction pattern of a Bragg grating with 50% duty cycle. (i) Measurement and (ii) simulation. Most of the intensity of the diffracted light is confined within the −1, 0, and + 1 orders. (b, c) Evolution of the diffraction pattern from the lens structure in Fig. 1(d), as measured at three different locations: (i) before, (ii) at focus and (iii) after focus, for (b) measured SH, (c) measured FF.

Optical Materials EXPRESS

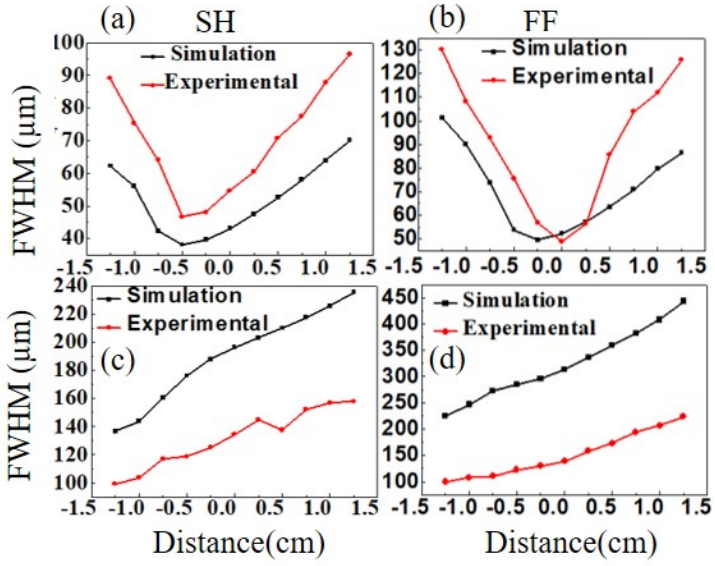

Fig. 5. Comparison of the beam radius for the converging (positive) diffraction order of (a) SH, (b) FF and diverging (negative) diffraction order of (c) SH, and (d) FF, as measured and simulated in Fig. 4. The measurement of the beam radius was performed in the horizontal direction and the beam is assumed rotationally symmetric.

Figure 3 illustrates the experimental optical setup to observe the beam shaping at SH and FF, respectively. The FF source used in the experiment was a Nd: YAG laser producing 10ns pulses at a 2kHz repetition rate. In order to shape the beam profile, the incident laser beam was focused on the exit face of the crystal using a 150mm focal length (L1) lens which produced waist radius around 200μm at 1064nm wavelength. This waist size ensures an illumination completely encompassing the binary structures with nearly constant transverse phase. The 4f lens system was used to image the shaped beam in the first order of diffraction to the camera. In this case, the lens (L2) of focal length 100mm was used for far-field imaging of beam-shapes at the camera. The SH beam was filtered out from FF by using a bandpass filter (FGS900, Thorlabs) whereas the FF beam was filtered out from SH by using 1064nm line filter of 10nm bandwidth (FL1064-10, Thorlabs).

For the Bragg grating structure (Fig. 1(c)), which has roughly 50% duty cycle, the diffraction pattern is shown in Fig. 4(a) with good agreement between Fig. 4(a, i) measurement and Fig. 4(a, ii) simulation. In this case, most of the incident power is diffracted into the 0, −1 and + 1 orders. The grating could be useful as a three-port beam splitter [19] for holography and interferometry [20]. Next, we measured the diffractive off-axis lens (Fig. 1(d)). The expression describing the binary structure is given in Table 1. A set of three measurements in different propagation distances form the focal series as shown in Fig. 4(b) for the SH and Fig. 4(c) for the FF.

Optical Materials EXPRESS

Table 1. Modulation expressions for desired beam profiles

Beam profile	Modulation expression
Off-axis lens (Fig. 1(d))	$sign[\cos(\frac{2\pi x}{\Lambda}+\frac{2\pi}{\lambda}\frac{(x^2+y^2)}{2F})]$
Fork grating (Fig. 1(e))	$sign[\cos(\frac{2\pi x}{\Lambda}+\phi)]$
Hermite-Gauss (HG_{12}) (Fig. 1(f))	$H_1(\frac{\sqrt{2}x}{w_0})\times H_2(\frac{\sqrt{2}y}{w_0})\times\exp(\frac{(x^2+y^2)}{{w_0}^2})$
2D Airy (Fig. 1(g))	$\frac{(x^3+y^3)}{3\beta^3}$

The expressions for: the off-axis lens and fork gratings; these are the exact binary modulations expressions assuming a π phase shift. Also, listed are the 2D cross section formulas for the Hermite-Gauss $_{12}$ and the two dimensional Airy beam; in this case, the beams were encoded into a binary structure using the method of Lee, as elaborated in the text. w_0 is the illumination beam waist (200μm at 1064nm), and (~27μm) is the nodal trajectory coefficient of the Airy beam. ϕ is the azimuthal phase.

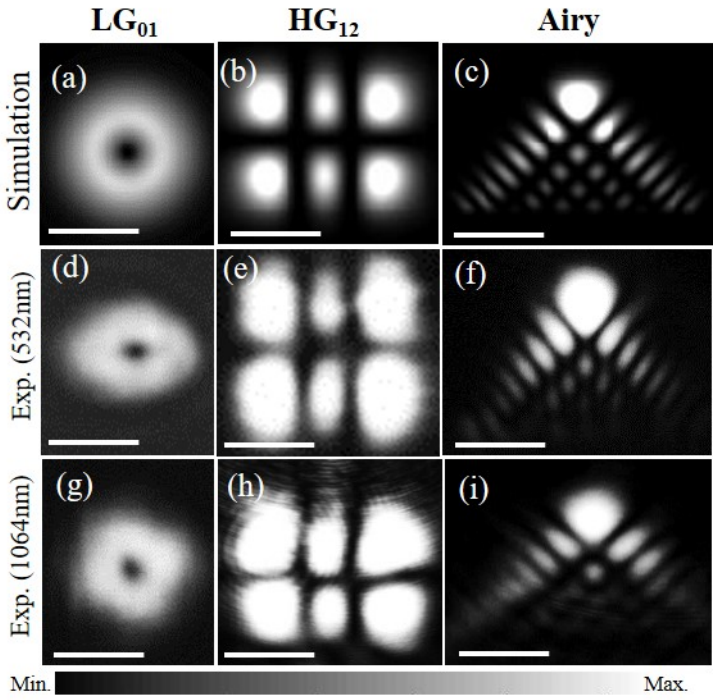

Fig. 6. Simulated (top row), experimental SH (middle row) and experimental FF (bottom row) results of (a) vortex beam, (b) HG_{12} and (c) Airy beam. The scale bar is 150μm.

The designed focal length was the F = 3cm in the first diffraction order of the FF, which translates to 1.5cm for the SH beam. As expected, in the positive first order a focusing lens is evident, while in the negative first order we find a defocusing lens. The diffraction pattern of the FF and SH also exhibit a two-dimensional sinc pattern, which is a result of the illuminating spot being larger than the square-shaped borders of the binary structure. Figure 5(a), Fig. 5(b) and Fig. 5(c), Fig. 5(d) compares the simulated and measured beam radius of the converging (positive) diffraction and diverging (negative) diffraction order, for the SH (Fig. 5(a), Fig. 5(c)) and FF (Fig. 5(b), Fig. 5(d)). Figure 6 shows the three different beam

Optical Materials EXPRESS

patterns, in the first order of diffraction: vortex beam, Hermite-Gauss $_{12}$ beam and the two-dimensional Airy beam. The expressions for these beams are given in Table 1; their encoding into a binary structure is done using the Lee method as elaborated on previously.

Figures 6(a)–6(c) shows the simulated beam shapes, Figs. 6(d)–6(f) and Figs. 6(g)–6(i) represent the experimentally observed beam shapes in SH and FF. The experimental results shown in Fig. 6 are in good agreement (>83-96%) for SH with the simulation results. The beam profiles at the pump wavelength are relatively less correlated (> 78-88%) since the structures were designed specifically for the second harmonic wavelength (modulations expressions assuming a π phase shift at SH wavelength). The generated beams were slightly different from the simulation because of the fabrication limitation, for example, owing to deviations of the milled patterns from the designed ones. We note that the small cracks that are seen in the masks for the Hermite-Gauss$_{12}$ and Airy beams, Fig. 1(f) and Fig. 1(g), did not reduce significantly the quality of the generated beams, since they are not periodic hence do not diffract efficiently into the first diffraction order. These cracks were caused by discharge during the e-beam writing, and can be eliminated by further optimizing the lithography process.

4. Conclusion

In this work, we have shown a new method for shaping beams in a nonlinear conversion process, by directly patterning the anti-reflection coating layer at the facet of an LBO nonlinear crystal. This is accomplished by ion-beam milling through a lithographically defined mask. The high damage threshold of LBO and the utilization of phase-only beam shaping offers important advantages for high power applications. The integration of beam shaping with the nonlinear crystal provides a compact device that can be used to modify and shape the incident fundamental beam and the nonlinearly generated beam for high power applications, and at wavelengths (e.g. in the ultraviolet) in which beam shaping elements such as spatial light modulator are not available. We have shown that multiple holograms can be generated on the same crystal facet, thus the same crystal can be utilized to generate different beam shapes by translating the pump beam. Finally, we note that the method we presented here can be further extended, using phase-only iterative design procedures such as Gerchberg Saxton's [21] for generating arbitrary shaped beams.

Funding

Israeli Science Foundation (1415/17); Israeli Innovation Authority.

Acknowledgement

DS acknowledges the support from the University Matching Fellowship, Tel Aviv University, Israel.